Journal of Materials Chemistry C

Accepted Manuscript

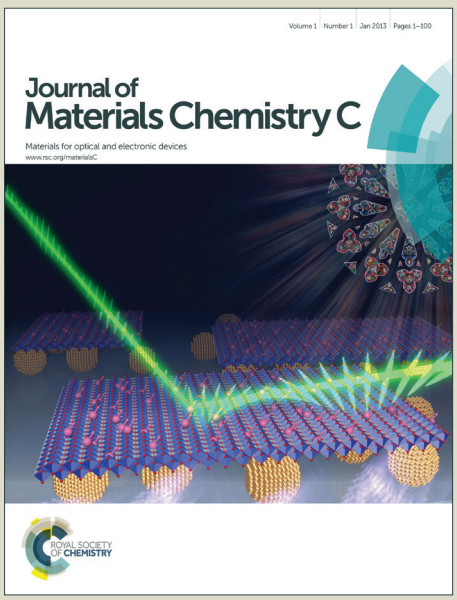

ROYAL SOCIETY OF CHEMISTRY

www.rsc.org/materialsC

Synthesis, Properties and Applications of Poly(ethylene glycol)-Decorated Tetraphenylethenes

Yilong Chen, Jacky W. Y. Lam, Sijie Chen, and Ben Zhong Tang

Table of contents entry

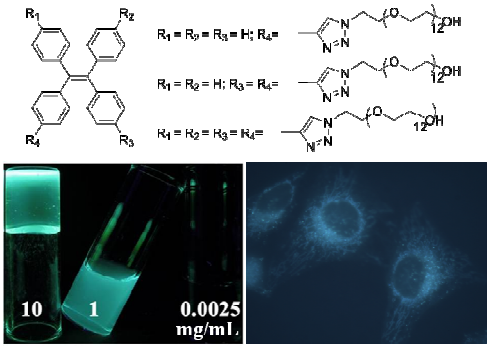

The properties and potential applications of non-charged, water soluble poly(ethylene glycol) (PEG)-decorated teraphenylethenes are investigated.

Journal Name

RSCPublishing

ARTICLE

Synthesis, Properties, and Applications of Poly(ethylene glycol)-Decorated Tetraphenylethenes

Cite this: DOI: 10.1039/x0xx00000x

Yilong Chen,[ab] Jacky W. Y. Lam,[ab] Sijie Chen,[ab] and Ben Zhong Tang*[abc]

Received 00th January 2014,
Accepted 00th January 2014

DOI: 10.1039/x0xx00000x

www.rsc.org/

Non-charged, water soluble poly(ethylene glycol) (PEG)-decorated teraphenylethenes (TPEs) with different polymer chain numbers are synthesized in high yields by azide-alkyne cycloaddition. Their aggregation and thermosensitive behaviours are investigated by means of fluorescence spectroscopy, transmission electron microscope (TEM), zeta potential and dynamic mechanical analyses. All the luminogenes are non-emissive in solutions, but emit intensely when aggregated in aqueous solutions, or forming micelles, demonstrating a phenomenon of aggregation-induced emission. TPE derivative (**1**) carrying one PEG chain forms hydrogels in THF/water mixture depending on concentration, water fraction and temperature. All the luminogens are thermosensitive, with their cloud point being tunable by varying the solvent composition and their hydrophilicity. Luminogen **1** is biocompatible and can function as a fluorescent visualizer for intracellular imaging.

Introduction

Since the observation of the phenomenon of aggregation-induced emission (AIE) in a series of propeller-shaped molecules, more than 100 research group in the world are now conducting the AIE research.[1-3] AIE luminogens are weakly emissive or non-fluorescent in solutions but are induced to emit efficiently by aggregate formation.[1] Such a characteristic enables them to find potential high-tech applications as chemosensors, bioprobes, immunoassay markers, stimuli-responsive materials and solid-state emitters.[1–3] Teraphenylethene (TPE) is a well-known AIE luminogen and enjoys the advantages of facile synthesis, efficient quantum yield in the solid state and high chemical and photo-stabilities. However, its hydrophobic nature greatly limits its biological applications. Physical mixing with water-soluble materials such as bovine serum albumin (BSA) or surfactants help improve its solubility or dispersion in aqueous medium.[2,3] Whereas this method enjoys the advantage of easy preparation, it trends to reduce the mechanical properties of the dye molecule and is difficult for quantification. Chemical incorporation of positively and negatively-charged groups is found to be effective to solve this problem. For example, TPE carrying two or four ammonium groups is water-soluble and emits weakly in aqueous solution. Its fluorescence is enhanced dramatically upon binding with calf thymus DNA or bovine serum albumin (BSA), making it to work as a fluorescence "turn-on" sensor for sensitive detection of biomolecules.[4,5] Electrostatic attraction or hydrophobic interaction of the TPE derivative with DNA and BSA, respectively, restricts the intramolecular rotation of the dye molecule, which blocks the nonradiative relaxation channel and hence enhances the light emission.

The thermal properties of polymers with a lower critical solution temperature (LCST) have been investigated extensively. These polymers possess both hydrophobic and hydrophilic groups and the balance between the two determines their LCST.[7,8] They are soluble or swell below the LCST in aqueous medium, but precipitate or shrink at temperature above the LCST. This property enables them to find possible applications in tissue engineering and controlled drug delivery. An example is represented by poly(*N*-isopropylacrylamide) (PNIPAM), whose temperature-induced conformational change can be sensitively followed by its functionalization with TPE.[9] Besides PNIPAM, poly(ethylene glycol) (PEG) is a well-known water-soluble polymer and becomes thermosensitive when melded with hydrophobic moieties.[10,11] PEG-containing amphiphilic macromolecules, on the other hand, can facilely self-assemble into micelles in aqueous solution. Biocompatible PEG-containing polymers are biomolecules approved by U.S. Food and Drug Administration, and are widely used to enhance the water solubility/dispersibility and biocompatibility of quantum dot, superparamagnetic iron oxide nanoparticles and drug carrying polymers for bioimaging and drug delivery.[12,13] PEG has also been reported to have non-specific interaction with biological substances to avoid immuno response and hence enhance non-specific cellular uptake. These features thus make it useful to improve the hydrophilicity of TPE and meanwhile impart the luminogen with thermosensitivity, self-assembly

property and good biocompatibility. However, such hybrid is rarely reported.[10]

In this work, we explored such possibility and synthesized water soluble, non-charged TPE derivatives with different PEG chain numbers via azide-alkyne cycloaddition. We found that TPE carrying one PEG chain (**1**) formed gels in THF/H_2O mixture, depending on concentration, water fraction and temperature. All the dye molecules form micelles at above the critical micelle concentration (CMC) and are thermosensitive. Luminogen **1** is biocompatible and can selectively image the cytoplasm of living cells.

Results and Discussion

Synthesis and Characterization. The PEG-decorated TPEs (**1**–**3**) were synthesized according to the synthetic routes shown in Scheme 1. PEG 600 with two hydroxy end groups was mono-tosylated by *p*-toluenesulfonyl chloride to afford **5**, which was further reacted with sodium azide to furnish **6**. Azide-alkyne cycloaddition of **6** with ethynyl-functionalized TPEs **7**–**9**, respectively, catalyzed by copper(I) bromide in the presence of PMDETA finally gave the desirable products **1**–**3** in high yields. All the compounds were characterized by standard spectroscopic methods and gave satisfactory analysis data corresponding to their molecular structures. For example, the IR spectrum shows a strong absorption band associated with the azide stretching vibration at 2107 cm^{-1}, which disappears upon its click reaction with **7** (Fig. 1A). Similarly, the C≡C−H and C≡C stretching vibrations of **7** occur at 3277 and 2108 cm^{-1}, which become invisible in the spectrum of **1**. All these suggest that the PEG chain has been successfully conjugated to the TPE core.

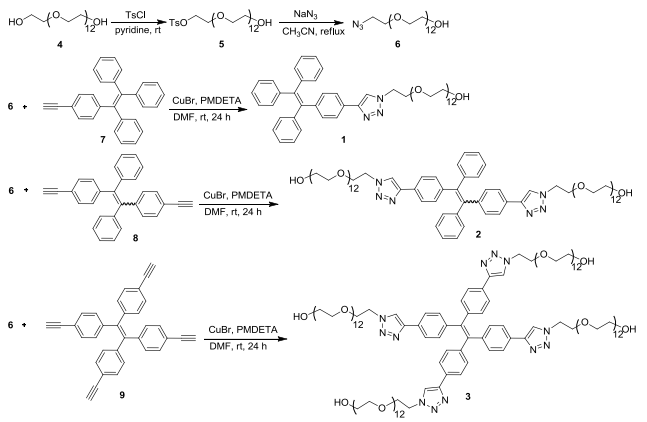

Scheme. 1 Synthesis of poly(ethylene glycol)-decorated tetraphenylethenes via azide-alkyne cycloaddition.

Similar results are obtained from the NMR analyses. The methylene protons (a) next to the azide group of **6** and methylene proton (e) of **7** resonate at δ 3.28 and 3.02, respectively, which shift to δ 4.59 (a') and 8.32 (e') after the click reaction due to the formation of triazole ring in **1** (Fig. 2). On the other hand, the spectrum of **1** shows no resonances of **7** at δ 76.8 and 83.1 (Fig. S1 in the Supporting Information).[14] New peaks emerge at the aromatic absorption region due to the cyclization of the azide group of **6** with the triple bond of **7** to form triazole rings in **1**.

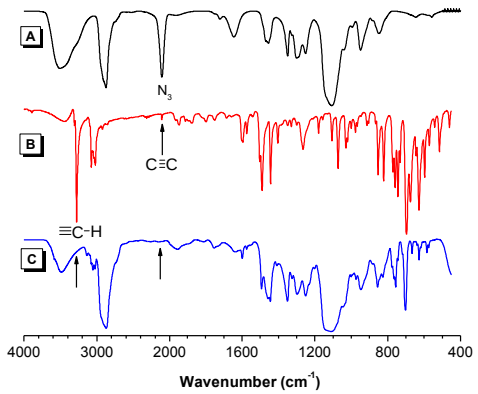

Fig. 1 IR spectra (A) **6**, (B) **7** and (C) **1**.

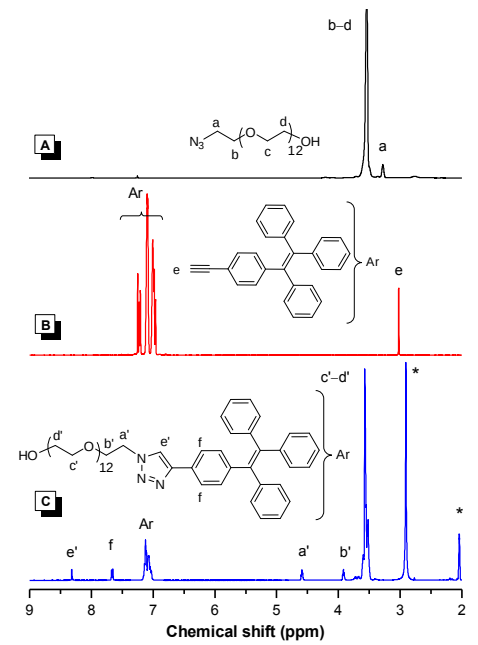

Fig. 2 ^{1}H NMR spectra of (A) **6** and (B) **7** in $CDCl_3$, and (C) **1** in $(CD_3)_2CO$.

Aggregation and Micellization. Fig. 3A shows the UV spectra of **1**–**3** in THF solutions. The absorption maximum of **1** is located at 350 nm, which is 50 nm red-shifted from that of unsubstituted TPE due to the electronic communication between the TPE core and the triazole ring. Increasing the number of triazole ring connected to the TPE core further red-shifts the UV spectrum: the absorption maximum of **2** and **3** occurs at 360 nm and 370 nm, respectively. The dilute THF solution of **1** emits almost no light upon photoexitation (Fig. 3B). The emission is still weak when less than 70% of water is added into the solution. Afterwards, it rises swiftly. At 95% water content, the PL intensity is 233-fold higher than that in pure THF solution. Since **1** possesses hydrophobic TPE unit, its molecules should aggregate in aqueous solution with a large

amount of water. Clearly, **1** inherits the property of TPE and is AIE-active. Similar phenomenon was also observed in **2** and **3** but the extent of emission enhancement upon aggregate formation is much less than that in **1**. For example, even at 100% water content or pure aqueous solution, the PL intensity of **2** and **3** increases only merely 175- and 8.5-fold, respectively. This is understandable as luminogens **2** and **3** contain more hydrophilic PEG chains and hence should possess higher solubility in aqueous solutions. Aggregates are thus less likely to be formed, thus resulting in weak AIE effect and hence emission.

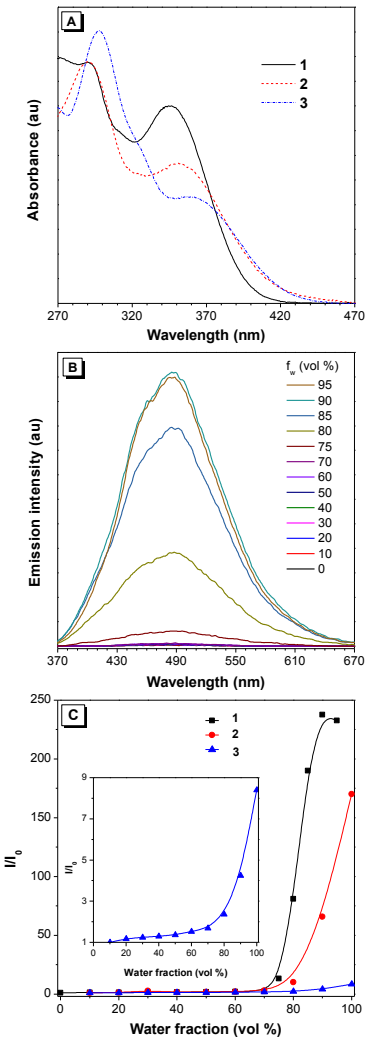

Fig. 3 (A) UV spectra of THF solutions of **1**–**3**. Concentration: 0.02 mg/mL. (B) PL spectra of **1** in THF and THF/H_2O mixtures with different water fractions (f_w). Concentration: 0.2 mg/mL; excitation wavelength: 350 nm. (C) Plot of relative PL intensity (I/I_0) versus the composition of the THF/H_2O mixtures of **1**–**3**. Concentration (mg/mL): 0.2 (**1**) and 3 (**2** and **3**). Excitation wavelength: 360 nm (**2**) and 370 nm (**3**) Inset: enlarged spectrum of **3**.

To study the micellization behaviours of the luminogens, the PL of their solutions with different concentrations was investigated at room temperature. Since the solubility of **1** in water is low, study on its micellization and gelation properties is performed in THF/water mixture. The PL intensity of **1**, for example, increases with increasing the solution concentration without causing any spectral change (Fig. 4A). The CMC can be calculated as the intersection point from the plot of relative PL intensity (I/I_0) against logarithm solution concentration (Figure 4B) and is determined to be 0.1, 0.4, and 0.6 mg/mL for **1**, **2** and **3**, respectively. It is noticeable that the CMC value increases with the number of PEG chains, suggesting that the luminogen becomes more hydrophilic when carrying more PEG chains. Gelation was observed at a concentration of above 5 mg/mL in **1**, which will be discussed in the next section.

Zeta potential analysis of THF/water mixtures (1:9 or 0:10 v/v) of **1**–**3** with a concentration of 1 or 3 mg/mL reveals particle size of 220.0, 85.7 and 55.6 nm with broad distribution and polydispersity of 0.3~0.4, respectively (Fig. 5). On the other hand, the TEM image of **1** shows spherical particles with diameters of ~150 nm (Fig. 6). All these suggest the formation of micelles with apolar TPE unit inside and hydrophilic PEG chains pointing to the medium. Below CMC, the luminogens are molecularly dissolved in the medium and shows no emission. Increasing the concentration above CMC induces the micelle formation and aggregates the TPE core, thus making the luminogens highly emissive.

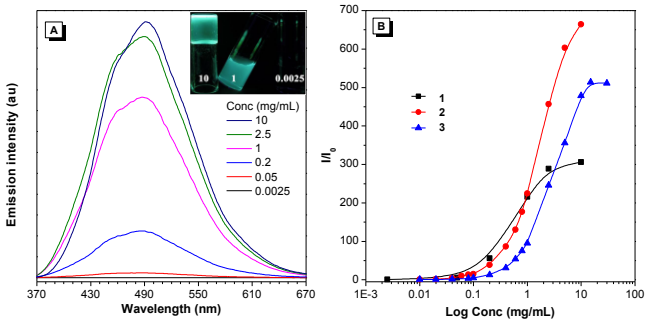

Fig. 4 (A) PL spectra of **1** in THF/H_2O mixtures (1:9 by volume) with different concentrations at room temperature. Inset: Photographs of THF/H_2O mixtures (1:9 by volume) of **1** with different concentrations taken under 365 nm UV irradiation. (B) Plots of relative intensity (I/I_0) versus logarithm concentration of **1** in THF/H_2O mixture (1:9 by volume) and **2** and **3** in water.

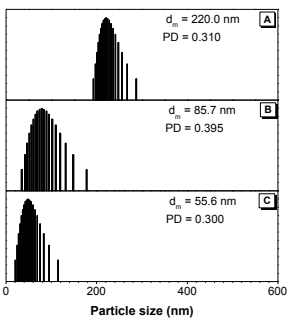

Fig. 5 Particle sizes of aggregates of (A) **1** formed in THF/H_2O mixture (1:9 by volume) and (B) **2** and (C) **3** formed in water. Concentration (mg/mL): 1 (**1**) and 3 (**2** and **3**).

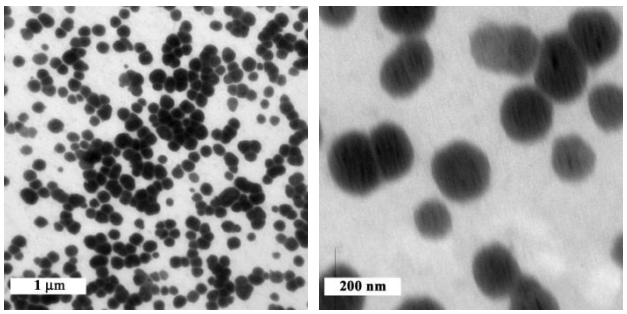

Fig. 6 TEM micrographs of **1** in THF/H_2O mixture (1:9 v/v) at different magnifications. Concentration: 1 mg/mL.

Sol-gel transition and thermosensitivity. Supramolecular gels have attracted great interest for their elegant architectures and potential high-tech applications in controlled drug release, template synthesis and biomimetics. To study the complicated gelator-gelator and gelator-solvent interactions, and sol-gel transition process, various detection techniques such as optical observation (transmittance and dropping ball methods) and thermal analysis have been developed. These methods, however, involve the use of bulky machines and measure a general outcome of samples, losing a lot of transition details. Fluorescence-based methods, on the other hand, enjoy the advantage of high sensitivity but are rarely utilized in studying the sol-gel transition, presumably due to the aggregation-induced quenching effect observed in some conventional fluorophores. However, the efficient emission of AIE luminogens in the aggregated state makes them promising for sol-gel transition study. Herein, we study the sol-gel transition and thermosensitivity of **1–3** using fluorescence spectroscopy.

In the previous section, we found that **1** formed gels at room temperature in THF/H_2O mixture (1:9 by volume) at a concentration of above 5 mg/mL. This means that below this concentration, the interactions between the gelators as well as gelators and solvent molecules are too weak to form qusi-solid self-assembly system. The amount of water required for gelation can be lowered by solution thickening. As shown in Fig. 7, the PL from an aqueous solution of **1** with a concentration of 10 mg/mL is still weak when the water content is below 75%. After then, the emission becomes stronger accordingly. The aqueous solution also starts to emit at 75% water content when doubling the solution concentration to 20 mg/mL, although a much higher PL enhancement was observed.

PEG is reported to be thermosensitive, showing LCST when attached to poly(ε-caprolactone). Similar behaviour was also observed in **1**–**3**, whose process can be followed by the temperature-dependent PL and transmittance analyses. The THF/H_2O mixture (3:7 v/v) of **1** with a concentration of 10 mg/mL is transparent. Its PL drops progressively with increasing the solution temperature and reaches the minimum intensity at 26 °C. Afterwards, the emission starts to drop again at ~45 °C (Fig. 8A). Thermal agitation generally brings dissolving effect and dehydration effects on the PL of **1**–**3**. The dissolving effect will enhance the molecular motion, leading to molecular separation and hence PL drop. The dehydration effect, on the other hand, will promote molecular aggregation, resulting in PL enhancement. The first one seems to be dominated at temperature below 26 °C or before the cloud point, while the first effect becomes more significant between 26 to 45 °C. After then, the effect of molecular motion prevails again and quenches the light emission gradually. The transmittance begins to fall at 29 °C, suggesting that the PEG chain starts to dehydrate. The cloud point determined at 50% transmittance is ~30 °C. Similar PL change was observed in gels of **1** formed in 90% aqueous solution with the same concentration but the cloud point now shifts to 59 °C. The transmittance, on the other hand, rises at 44 °C but drops again at ~60 °C. We believe the first change is caused by gel to sol transition of the dye molecule, while the second one is caused by the dehydration of the PEG chain. The sol-gel transition is reversible and gelation occurs upon cooling the solution to lower temperatures. The PL of a less concentrated solution with the same composition, on the hand, decreases monotonically due to the predominance of the dissolving effect on the light emission process by heating even the PEG chain dehydrates and aggregates at the cloud point. The cloud point was found to locate at 57 °C from the transmittance measurement. These results show that the solvent composition exerts a stronger effect on the cloud point than the solution concentration. Similar phenomena are observed in **2** and **3**. Since they are more hydrophilic than **1**, their cloud points occur at higher temperatures of 49 °C and 74 °C, respectively. Compared with the transmittance analysis, more information is provided by the fluorescence method. Thus, AIE fluorophores are promising in phase transition study.

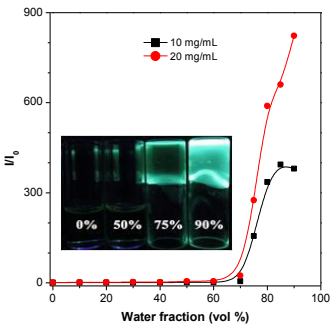

Fig. 7 Plot of relative intensity (I/I_0) versus the water fraction in THF/H_2O mixtures of **1** with concentrations of 10 and 20 mg/mL. Inset: Photographs of THF/H_2O mixtures of **1** (10 mg/mL) with different water fractions taken under 365 nm UV irradiation.

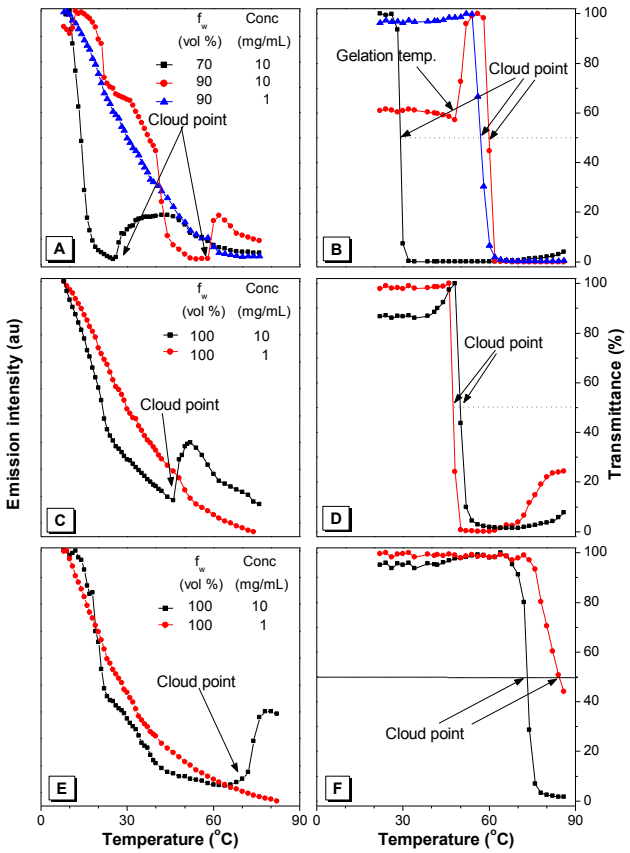

Fig. 8 Plots of (A, C and E) PL intensity and (B, D and E) transmittance against temperature in THF/H_2O mixtures of (A and B) **1**, (C and D) **2** and (E and F) **3** with different water fractions (f_w) and concentrations. Excitation wavelength (nm): 350 (**1**), 355 (**2**) and 360 (**3**).

The mechanical properties of **1** are investigated by rheometric method. As shown in Fig. 9A, the gel with elastic modulus (G') of 3 Pa and viscous modulus (G") of 0.5 Pa is mechanically stable at 25 °C and changes little with time. The G' and G" increase upon heating and reach their maximum value of 40 Pa and 20 Pa, respectively, at ~50 °C. Afterwards, they drop dramatically due to gel to sol transition and dehydration.

As stated before, **1** forms micelle in aqueous solution with an appropriate concentration. The micelles interpenetrate to each other upon solution thickening and finally gels are formed. No gels are formed in **2** and **3** even at very high solution concentration, presumably due to their higher hydrophilicity as they possess a larger number of PEG chains. In order to form micelles, their PEG chains have to be bent. This gives rise in a twisted molecular conformation that may hamper gel formation. Thus, both the molecular structure and the balance between hydrophilicity and hydrophobicity of a dye molecule play important roles in its gel formation.

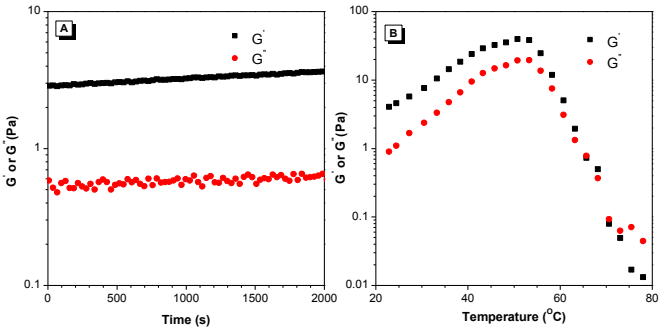

Fig. 9 Changes in elastic modulus (G') and viscous modulus (G") of gels of **1** formed in THF/H_2O mixture (1:9 v/v; 10 mg/mL) with (A) time at 25 °C, frequency of 1 Hz and strain of 5% and (B) temperature at a heating rate of 5 °C/min.

***In Vitro* Cell Imaging.** Prior to the cell imaging, the cell viability or cytotoxicity of luminogen **1** was evaluated in HeLa cells using MTT assay. The cell were exposed to varying concentration (0, 2.5, 5, 7.5, 10 μg/mL) of **1** for 24 h in CO_2 incubator at 37 ℃ for cell proliferation (Fig. 10). The result shows that luminogen **1** is generally noncytotoxic at the concentration even up to 10 μg/mL. The efficient PL of AIE dyes in the aggregated state makes them promising as fluorescent visualizers for intracellular imaging. However, they are normally hydrophobic and suffer low solubility in physiological medium. Some water soluble AIE dyes with charged groups have been prepared and can selectively stain the cytoplasm and mitochondrion of living cells. Non-charged water soluble AIE dyes, on the other hand, are seldom reported. Luminogen **1** is amphiphilic and possesses such capability. As shown in Fig. 11, the dye molecule stains the cytoplasmic region of HeLa Cells but not their nucleic parts. The dye molecule may also stain the mitochondria, as some bright filamentous structures are observed. Because of its amphiphilic nature, it is likely that the aggregates of **1** enter other membrane-bound organelles such as endoplastic reticula.

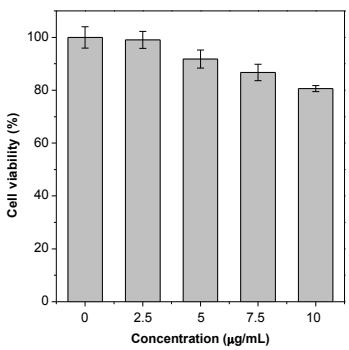

Fig. 10 Effect of **1** on cell proliferation of HeLa cells evaluated by MTT assay. The cells were exposed to various concentrations of **1** for 24 h.

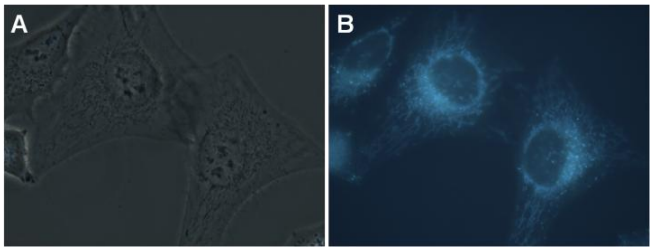

Fig. 11 (A) Bright-field and (B) fluorescent images of living HeLa cells stained with 5.2 μg/mL of **1**.

Conclusions

In this work, water soluble AIE luminogens are synthesized in high yields using the technique of azide-alkyne cycloaddition. These luminogens are non-emissive in solutions but emit intensely when aggregated, displaying a novel AIE phenomenon. Under appropriate concentration, composition and temperature, **1** forms gels in THF/water mixture. All the luminogens are thermosensitive, with their cloud point being tunable by the solvent composition and their hydrophilicity. Luminogen **1** is cytocompatible and can function as a fluorescent visualizer for intracellular imaging.

Experimental

Materials. 1-(4-Ethynylphenyl)-1,2,2-triphenylethene (**7**), 1,2-bis(4-ethynylphenyl)-1,2-diphenylethene (**8**) and 1,1,2,2-tetrakis(4-ethynylphenyl)ethene (**9**) were synthesized according to the literature methods.[14] Poly(ethylene glycol) (M_n = 600), *p*-toluenesulfonyl chloride (TsCl), pyridine, sodium azide, copper(I) bromide, pentamethyldiethylenetriamine (PMDETA) and other chemicals and solvents were all purchased from Aldrich and used as received without further purification. Distilled water was used throughout the experiments.

Instruments. ^{1}H and ^{13}C NMR spectra were measured on a Bruker ARX 400 NMR spectrometer using $CDCl_3$ or $(CD_3)_2CO$ as solvent and TMS as internal standard. FTIR spectra were recorded on a Bruker spectrophotometer (Tensor 27). The weight-average molecular weight (M_w) and polydispersity indices (PDI or M_w/M_n) of the luminogens were estimated by a Waters Associates gel permeation chromatography (GPC) system equipped with RI, UV and fluorescence detectors using THF as eluent and polystyrenes as standard. UV-vis absorption spectra were recorded on a Cary 50 Conc UV visible spectrometer and the transmittance measurements were carried out on a UV/VIS/NIR spectrophotometer (Bruker, Lambda 900) at a wavelength of 550 nm. Photoluminescence (PL) spectra were recorded on a Perkin-Elmer spectrofluorometer LS 55. The temperature control was achieved by placing the sample in a cell compartment connected to water circulation system. Water from a thermostated bath was allowed to circulate through the walls of the sample compartment. The final temperature of the sample was measured on a digital thermometer (TES, TES-1310). The particle sizes were measured on a zeta potential analyzer (Brookhaven, ZETAPLUS). To prepare an unstained specimen for transmission electron microscope (TEM) analysis, a drop of the sample was placed on a carbon-coated copper grid for 2 min. The excess solution was blotted with filter paper. After drying the grid samples in air, TEM images were taken on a TEM instrument (Japan, JEOL JEM 100CXII) with a camera set at an accelerating voltage of 100 kV. Rheological characterization of the gel was performed by using a Rheometric ARES 3 system with 50 mm parallel plate geometry. In order to avoid solvent evaporation, the surface of the sample between two plates was covered with glycerol. The evolution of moduli (G' and G'') versus time was tested at 25 °C with a frequency of 1 Hz and a strain of 5%. The temperature ramp was measured a 1 Hz frequency and a strain of 5% at a heating rate of 5 °C/min. For cell imaging experiment, HeLa cells were grown overnight on a plasma-treated 25 mm round cover slip mounted onto a 35 mm Petri dish with an observation window. The living cells were stained with **1** (5.2 μg/mL) for 4 h. The cells were imaged under an inverted fluorescence microscope (Nikon Eclipse TE2000-U) using a combination of excitation and emission filters: λ_{ex} = 330–380 nm. The images of the cells were captured using a computer-controlled SPOT charge-coupled device (CCD) camera (SPOT RT SE 18 Mono). HeLa cells were seeded into a 96-well plate at a density of 8×10^3 per well overnight before treated with compound **1** in different concentrations. The cell proliferation was measured using MTT assay according to the manufacturer's instructions. After 24 h incubation in incubator, the cells were washed three times with 1× PBS. After that, 10 μL of 3-(4,5-dimethyl-2-thiazolyl)-2,5-diphenyltetrazolium bromide (MTT) solution (5 mg/mL in phosphate buffer solution) was added into the each well. After 4 h incubation at 37 °C, 100 μL of solubilization solution containing 10% SDS and 0.01 M HCl was added to dissolve the purple crystals. After 8 h incubation, the optical density readings at 595 nm were taken using a plate reader. Each of the experiments was performed at least 3 times.

Synthesis of PEG 600 mono-tosylate (5). To a pyridine (60 ml) solution of **4** (16.00 mmol) was added TsCl (6.10 g, 32.00 mmol) and the mixture was stirred at room temperature for 2–3 h. The reaction mixture was diluted with dichloromethane (DCM) (200 mL), washed with aqueous 1 M HCl (100 mL), 4% $NaHCO_3$ solution and brine, and dried over anhydrous Na_2SO_4. After solvent evaporation, the residue was purified on a silica-gel column with methanol/DCM mixture (1:10 v/v) as eluent. Yield 76%. IR (KBr), ν (cm^{-1}): 3436, 2873, 1664, 1456, 1352, 1296, 1250, 1176, 1110, 923, 820, 777, 665, 554. ^{1}H NMR (400 MHz, $CDCl_3$), δ (ppm): 7.79 (2H, t, J = 8.0 Hz, Ts-H), 7.34 (2H, t, J = 8.0 Hz, Ts-H), 4.15 (2H, t, J = 4.8 Hz, $TsOCH_2$), 3.77–3.54 (50H, m, OCH_2), 2.43 (3H, d, Ts-CH_3).

Synthesis of PEG 600 mono-azide (6). To an acetonitrile (150 ml) solution of **5** (12.00 mmol) was added sodium azide (1.17 g, 18.00 mmol). After reflux for 32 h and cool to room temperature, the mixture was diluted with water (200 mL). The aqueous solution was extracted with dichloromethane four times. The combined organic phases were dried over anhydrous Na_2SO_4. After solvent evaporation, the residue was purified on a silica-gel column using methanol/DCM (1:10 v/v) as eluent. Yields 95%. IR (KBr) ν (cm^{-1}): 3497, 2873, 2107, 1644, 1455, 1350, 1293, 1251, 1108, 948, 845.^{1}H NMR (400 MHz, $CDCl_3$)

δ (ppm): 3.77–3.44 (50H, m, OCH_2), 3.28 (2H, t, J = 5.0 Hz, N_3CH_2).

Synthesis of TPE derivatives 1–3. Luminogen **1** was synthesized with the reagent feed ratio [**6**]/[**7**]/[CuBr]/[PMDETA] of 1/1.1/1.1/1.1. While for **2** and **3**, a feed ratio [**6**]/[**8**]/[**9**] of 1.1/1/1 was used instead. The click reaction between **6** (469 mg, 0.75 mmol) and **7** (294 mg, 0.825 mmol) was conducted at 35 °C in a 50 mL Schlenk flask with 30 mL of DMF, CuBr (118.4 mg, 0.825 mmol) and 3.65 mL PMDETA (0.825 mmol). After stirring for 36 h, the reaction mixtures were diluted with water (300 mL) and the aqueous solution was extracted with dichloromethane four times. The combined organic phases were further washed with brine six times and dried over Na_2SO_4. After solvent evaporation, the residue was purified on a silica-gel column using DCM as eluent to give the corresponding product in a yield of 92%. For **2** and **3**, the filtrates were condensed to 10 mL and then precipitated in ethyl ether three times. All the products were purified and characterized by GPC and FTIR, ^{1}H NMR and ^{13}C NMR spectroscopies.

Luminogen **1**. Yield 92%. M_w 1100; M_w/M_n 1.3. IR (KBr), ν (cm^{-1}): 3484, 3055, 2871, 1950, 1752, 1598, 1493, 1446, 1351, 1298, 1251, 1112, 1045, 947, 855, 825, 756, 703, 666, 627, 585. ^{1}H NMR (400 MHz, $(CD_3)_2CO$), δ (ppm): 8.32 (1H, s, triazole-H), 7.66 (2H, d, J = 7.6 Hz, triazole-Ar-H), 7.14–7.02 (17H, m, Ar-H), 4.59 (2H, t, J = 4.8 Hz, CH_2-triazole), 3.92 (2H, t, J = 4.8 Hz, OCH_2CH_2-triazole), 3.60–3.51 (48H, m, OCH_2). ^{13}C NMR (100 MHz, $(CD_3)_2CO$), δ (ppm): 147.42, 144.62, 144.02, 142.13, 141.66, 132.44, 132.03, 130.60, 128.65, 127.46, 125.59, 122.22, 73.58, 71.18, 70.12, 62.00, 50.89.

Luminogen **2**. Yield 85%. M_w 2100; M_w/M_n 1.3. IR (KBr), ν (cm^{-1}): 3418, 3020, 2866, 2111, 1645, 1469, 1392, 1351, 1300, 1249, 1118, 971, 926, 844, 805. ^{1}H NMR (400 MHz, $(CD_3)_2CO$), δ (ppm): 8.33 (2H, s, triazole-H), 7.68 (4H, t, J = 7.4 Hz, triazole-Ar-H), 7.13–7.05 (14H, m, Ar-H), 4.59 (4H, t, J = 4.8 Hz, CH_2-triazole), 3.91 (4H, t, J = 4.8 Hz, OCH_2CH_2-triazole), 3.60–3.51 (96H, m, OCH_2). ^{13}C NMR (100 MHz, $(CD_3)_2CO$), δ (ppm): 147.43, 144.54, 144.09, 141.83, 132.51, 132.09, 130.09, 128.80, 127.61, 125.71, 122.38, 73.62, 71.27, 70.11, 61.97, 51.43, 50.90.

Luminogen **3**. Yield 82%. M_w 3600; M_w/M_n 1.3. IR (KBr), ν (cm^{-1}): 3428, 3136, 2869, 2105, 1645, 1459, 1350, 1297, 1250, 1109, 972, 946, 843, 807. ^{1}H NMR (400 MHz, $(CD_3)_2CO$), δ (ppm): 8.33 (4H, s, triazole-H), 7.70 (8H, d, J = 7.2 Hz, triazole-Ar-H), 7.17 (14H, J = 7.2 Hz, d, Ar-H), 4.57 (8H, s, CH_2-triazole), 3.89 (8H, s, OCH_2CH_2-triazole), 3.60–3.40 (192H, m, OCH_2). ^{13}C NMR (100 MHz, $(CD_3)_2CO$), δ (ppm): 147.43, 144.01, 141.67, 132.67, 130.78, 125.81, 122.51, 73.61, 70.72, 70.11, 61.95, 51.43, 50.92.

Acknowledgements

This work was partially supported by National Basic Research Program of China (973 Program; 2013CB834701), the Research Grants Council of Hong Kong (604711, 602212, HKUST2/CRF/10, and N_HKUST620/11), the Innovation and Technology Commission (ITCPD/17-9), and the University Grants Committee of Hong Kong (AoE/P-03/08 and T23-713/11-1). B.Z.T. thanks the support from Guangdong Innovative Research Team Program (201101C0105067115).

Notes and references

[a]HKUST Shenzhen Research Institute, No. 9 Yuexing 1st RD, South Area, High-tech Park, Nanshan, Shenzhen 518057, China. E-mail: tangbenz@ust.hk
[b]Department of Chemistry, Institute for Advanced Study, Division of Life Science, Institute of Molecular Functional Materials, Division of Biomedical Engineering and State Key Laboratory of Molecular Neuroscience, HKUST, Clear Water Bay, Kowloon, Hong Kong, China
[c]Guangdong Innovative Research Team, SCUT-HKUST Joint Research Laboratory, State Key Laboratory of Luminescent Materials and Devices, South China University of Technology, Guangzhou 510640, China

†Electronic Supplementary Information (ESI) available: IR, ^{1}H NMR and ^{13}C NMR spectra of **1**–**3**. See DOI: 10.1039/b000000x/

1 (a) J. Luo, Z. Xie, J. W. Y. Lam, L. Cheng, H. Chen, C. Qiu, H. S. Kwok, X. Zhan, Y. Liu, D. Zhu, B. Z. Tang, *Chem. Commun*. 2001, **18**, 1740; (b) B. Z. Tang, X. Zhan, G. Yu, P. P. S. Lee, Y. Liu, D. Zhu, *J. Mater. Chem.*, 2001, **11**, 2974; (c) Y. Hong, J. W. Y. Lam, B. Z. Tang, *Chem. Commun.* 2009, 4332; (d) Y. Hong, J. W. Y. Lam, B. Z. Tang, *Chem. Soc. Rev.*, 2011, **40**, 5361; (e) D. Ding, K. Li, B. Liu, B. Z. Tang, *Acc. Chem. Res.* 2013, **46**, 2441; (f) S. J. Yoon, J. H. Kim, K. S. Kim, J. W. Chung, B. Heinrich, F. Mathevet, P. Kim, B. Donnio, A. J. Attias, D. Kim, S. Y. Park, *Adv. Funct. Mater.* 2012, **22**, 61; (g) N. B. Shustova, A. F. Cozzolino, S. Reineke, M. Baldo, M. Dincă, *J. Am. Chem. Soc.* 2013, **135**, 13326; (h) J. Huang, X. Yang, J. Wang, C. Zhong, L. Wang, J. Qin, Z. Li, *J. Mater. Chem.* 2012, **22**, 2478.

2 W. Qin, D. Ding, J. Z. Liu, W. Z. Yuan, Y. Hu, B. Liu, B. Z. Tang, *Adv. Funct. Mater.*, 2012, **22**, 771.

3 (a) K. Li, Y. H. Jiang, D. Ding, X. Zhang, Y. T. Liu, J. L. Hua, S. S. Feng, B. Liu, *Chem. Commun.*, 2011, **47**, 7323; (b) D. Ding, K. Li, W. Qin, R. Y. Zhan, Y. Hu, J. Z. Liu, B. Z. Tang, B. Liu, *Adv. Healthcare Mater.*, 2013, **2**, 500.

4 H. Tong, Y. Hong, Y. Q. Dong, M. Haussler, J. W. Y. Lam, Z. Li, Z. F. Guo, Z. H. Guo, B. Z. Tang, *Chem. Commun.*, 2006, 3705.

5 Y. Hong, M. Haussler, J. W. Y. Lam, Z. Li, K. K. Sin, Y. Q. Dong, H. Tong, J. Z. Liu, A. J. Qin, R. Renneberg, B. Z. Tang, *Chem.–Eur. J.*, 2008, **14**, 6428.

6 H. Tong, Y. Hong, Y. Q. Dong, M. Haeussler, Z. Li, J. W. Y. Lam, Y. P. Dong, H. H. Y. Sung, I. D. Williams, B. Z. Tang, *J. Phys. Chem. B*, 2007, **111**, 11817.

7 (a) N. A. Platé, T. L. Lebedeva, L. I. Valuev, *Polym. J.*, 1999, **31**, 21; (b) H. Y. Liu, X. X. Zhu, *Polymer*, 1999, **40**, 6985; (c) Y. Chen, J. E. Gautrot, X. X. Zhu, *Langmuir*, 2007, **23**, 1047.

8 K. Iwai, Y. Matsumura, S. Uchiyama, A. P. Silva, *J. Mater. Chem.*, 2005, **15**, 2796.

9 L. Tang, J. K. Jin, A. Qin, W. Z. Yuan, Y. Mao, J. Mei, J. Z. Sun, B. Z. Tang, *Chem. Commun.*, 2009, 4974.

10 (a) C. Y. Gong, S. Shi, P. W. Dong, B. Kan, M. L. Gou, X. H. Wang, X. Y. Li, F. Luo, X. Zhao,Y. Q. Wei, Z. Y. Qian, *Int. J. Pharm.*,

2009, **365**, 89; (b) X. Yin, F. Meng, L. Wang, *J. Mater. Chem. C*, 2013, **1**, 6767.

11 (a) A. J. Dong, Y. L. Zhai, L. Xiao, H. Y. Qi, Q. Tian, L. D. Deng, R. W. Guo, *J. Polym. Sci. Part A: Polym. Chem.*, 2010, **48**, 503; (b) L. N. Goswami, Z. H. Houston, S. J. Sarma, S. S. Jalisatgi, M. F. Hawthorne, *Org. Biomol. Chem.*, 2013, **11**, 1116.

12 A. C. Albertsson, I. K. Varma, *Biomacromolecules*, 2003, **4**, 146.

13 F. Couet, N. Rajan, D. Mantovani, *Macromol. Biosci.*, 2007, **7**, 701.

14 R. R. Hu, J. W. Y. Lam, J. Z. Liu, H. H. Y. Sung, I. D. Williams, Z. N. Yue, K. S. Wong, M. M. F. Yuen, B. Z. Tang, *Polym. Chem.*, 2012, **3**, 1481.

